

Reflectance-difference spectroscopy of (001) GaAs surfaces in ultrahigh vacuum

Itaru Kamiya*

Bellcore, 331 Newman Springs Road, Red Bank, New Jersey 07701-7040

and Department of Physics, University of Illinois at Urbana-Champaign, Urbana, Illinois 61801

D. E. Aspnes,[†] L. T. Florez, and J. P. Harbison

Bellcore, 331 Newman Springs Road, Red Bank, New Jersey 07701-7040

(Received 19 June 1992)

Reflectance-difference spectroscopy (RDS) is employed to study *in situ* the (4×2) , (1×6) , (4×6) , (3×1) , $(2\times 4)\text{-}\alpha$, $(2\times 4)\text{-}\beta$, $(2\times 4)\text{-}\gamma$, $c(4\times 4)$, and $d(4\times 4)$ reconstructions of (001) GaAs surfaces prepared in ultrahigh vacuum (UHV) by molecular-beam epitaxy and simultaneously characterized by reflection high-energy electron diffraction (RHEED). Reproducibility of the data is excellent. With the aid of previous theoretical calculations, we interpret characteristic spectral features at 1.9, 2.6, and 4.2 eV in terms of electronic excitations involving surface dimers of Ga, As, and As, respectively. Because RD couples to local electronic structure rather than to long-range order, RD spectra not only determine surface reconstructions but also provide details not accessible by RHEED, such as the existence of As dimers in the (1×6) , (4×6) , and (3×1) reconstructions and of the fractional coverage within a given reconstruction. Our data show that the (3×1) , (1×6) , and (4×6) reconstructions are at least partly determined by kinetics, since they can only be obtained by following specific heating or cooling procedures under very low As_4 flux. More generally, it is possible to employ this optical technique to determine surface atomic and electronic structure. Because RD spectra can be obtained with the surface in any transparent ambient, the database that we have established here provides a new approach for elucidating surface reconstructions of (001) GaAs and hence the dynamics of surface reactions in non-UHV environments.

I. INTRODUCTION

The (001) GaAs surface has attracted much attention during the past few decades for both technological and scientific reasons. As shown by diffraction probes such as reflection high-energy electron diffraction (RHEED), (001) GaAs exhibits a variety of reconstructions depending on substrate temperature and surface stoichiometry.¹⁻⁸ With increasing As coverage the surface exhibits long-range orderings (LRO's) of $c(4\times 4)$, (2×4) , (3×1) , (1×6) , (4×6) , and (4×2) . Transitional phases and subsets of reconstructions within these LRO's have also been reported.

These reconstructions have been most thoroughly investigated by RHEED,^{1,2} which is currently the primary method of establishing the state of the surface during crystal growth by molecular-beam epitaxy (MBE).^{3,4} Detailed studies have also been carried out on MBE-prepared surfaces by low-energy electron diffraction (LEED),^{5,6} Auger electron spectroscopy (AES),^{5,6} and photoemission spectroscopy (PES).^{6,8} However, these conventional tools have provided only indirect information on the real-space atomic structure of the surface. More direct information has recently been provided by scanning tunneling microscopy (STM).^{9,10} With the aid of complementary measurements by RHEED, LEED, PES or x-ray diffraction (XRD),¹¹ STM has confirmed the existence of dimers and many of the speculated atomic arrangements. While STM would therefore seem to be the optimum probe for studying surface atomic structure,

the tip needs to be located very near the surface, which causes difficulties in application in *in situ* dynamic studies. In addition, if the electronic structure of the surface is drastically perturbed, as for example by adsorbates, the interpretation of images is not always straightforward.¹²⁻¹⁶

Epitaxial growth by MBE or organometallic chemical vapor deposition (OMCVD) takes place at substrate temperatures of 400–700 °C with reactive species being continuously supplied to the surface. These conditions are incompatible with all the above-mentioned probes, except for RHEED and XRD. Unfortunately, RHEED can only be used in high vacuum, and both RHEED and XRD couple to LRO, not to local electronic structure. Therefore, to obtain information about the local electronic and atomic structure under dynamic conditions, new approaches are required.

Optical probes, including reflectance difference spectroscopy (RDS),¹⁷⁻¹⁹ laser light scattering (LLS),²⁰ surface photoabsorption (SPA),²¹ spectroscopic ellipsometry (SE),²² second-harmonic generation (SHG),²³ sum-frequency generation (SFG),²⁴ and various infrared (IR) spectroscopies,²⁵ are now being developed to meet this need. These probes are nondestructive, noninvasive, and can be used in any transparent ambient. However, optical probes have not been a major factor in surface analysis because photons interact relatively weakly with material, which results in a low surface sensitivity. To compensate for this low sensitivity, the recent trend has been to take advantage of symmetry in some way to

enhance the contribution of the surface relative to the dominant but uninteresting contribution from the bulk. For example, LLS and SPA deal with nonspecular scatter and the Brewster-angle reflectance of *p*-polarized light, respectively. These probes have been employed extensively for kinetic investigations of OMCVD processes because their instrumental requirements are relatively simple. However, they have not been satisfactory for the analysis of electronic and atomic structure. SHG and SFG depend on the lower symmetry of the surface to generate harmonic components of an intense incident beam that cannot be generated in the bulk. These approaches provide useful symmetry information with excellent time resolution but in their present forms are complicated and do not possess significant spectroscopic capabilities. SE is more accurately described as a bulk probe that is affected by surface conditions. Therefore, it is most suited for the study of surface transients. IR spectroscopies do not directly resolve atomic structures, although they have recently demonstrated their potential for identifying adsorbates and establishing the bonding configurations of the adsorbates.²⁵

However, RDS has recently proven its capability for studying the structure of both steady and transient surfaces in various environments, for example UHV,¹⁷ atmospheric pressure (AP) gases,^{18,19,26-28} and even liquids.²⁹ RDS takes advantage of the fact that the bulk dielectric responses of cubic materials are essentially isotropic, so any anisotropy that is detected comes primarily from the surface. Using RDS, we have shown that (001) GaAs surfaces in AP H₂, He, and N₂ exhibit reconstructions similar or identical to those in UHV.²⁷ However, these results could only be achieved by first obtaining reference spectra on well-defined surfaces prepared in UHV. In the present work, we provide a detailed description of how this RD database was obtained and extend it to other (001) GaAs reconstructions in UHV.

II. EXPERIMENT

The principle and methods of RDS have been described elsewhere.¹⁷ The spectrometer is constructed from the following: a 75-W Xe short-arc lamp, front-surface spherical and plane mirrors, MgF₂ and quartz Rochon polarizers, a 50-kHz photoelastic modulator, a 0.1-m focusing-grating monochromator with 0.5-mm slits, and an extended S-20 photomultiplier detector. These components are all mounted on a 16×12-in² Al plate, as shown in Fig. 1.³⁰ Under typical conditions a spectrum from 1.5 to 5.5 eV is obtained in 25 s.

For (001) GaAs the measured quantity is the relative difference between the complex near-normal-incidence reflectances $\tilde{r}_{\bar{1}10}$ and \tilde{r}_{110} of light linearly polarized along the two principle axes $[\bar{1}10]$ and $[110]$, respectively:

$$\frac{\Delta\tilde{r}}{\tilde{r}} = \frac{\Delta r}{r} + i\Delta\theta = \frac{(\tilde{r}_{\bar{1}10} - \tilde{r}_{110})}{\tilde{r}}, \quad (1)$$

where

$$\tilde{r} = \frac{\tilde{r}_{\bar{1}10} + \tilde{r}_{110}}{2}. \quad (2)$$

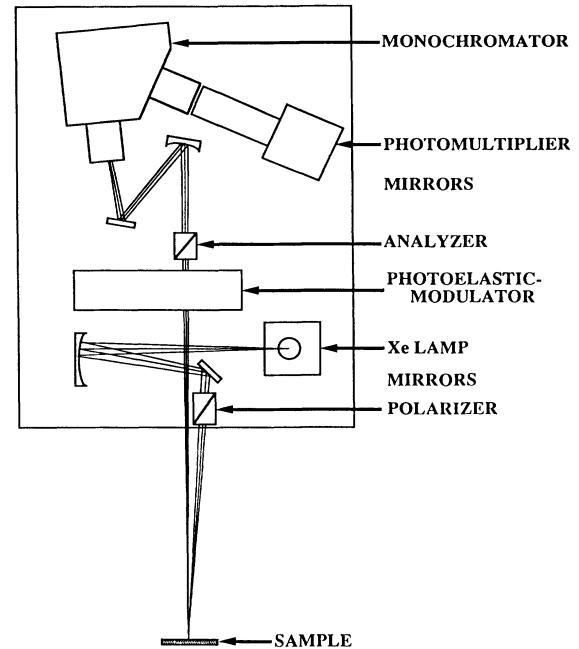


FIG. 1. Schematic diagram of the RD spectrometer employed in the present study.

The two-prism photoelastic-modulator configuration allows us to measure both relative amplitude $\Delta r/r$ and phase $\Delta\theta$ of the anisotropy of the complex reflectance. In the Fresnel three-phase model $\Delta\tilde{r}/\tilde{r}$ can be expressed in terms of the surface dielectric anisotropy $(\epsilon_{\bar{1}10} - \epsilon_{110})d$ as³¹

$$\frac{\Delta\tilde{r}}{\tilde{r}} = \frac{4\pi id}{\lambda} \frac{\epsilon_{\bar{1}10} - \epsilon_{110}}{\epsilon_s - 1}, \quad (3)$$

where ϵ_s is the bulk dielectric function of GaAs, $\epsilon_{\bar{1}10}d$ and $\epsilon_{110}d$ are the surface dielectric responses along the $[\bar{1}10]$ and $[110]$ axes, respectively, and λ is the wavelength of the light. For $\text{Im}(\epsilon_s) \ll \text{Re}(\epsilon_s)$ the imaginary part of $(\epsilon_{\bar{1}10} - \epsilon_{110})d$ is related to the anisotropy of the surface absorption. In this case, which applies to all semiconductors for energies below the E_1 threshold, the real part of $\Delta\tilde{r}/\tilde{r}$ will be dominated by the surface absorption properties. Because $\Delta r/r$ is also relatively free from experimental artifacts such as effects due to strain birefringence of the UHV viewing ports, we use $\Delta r/r$ throughout.

Since GaAs is a cubic material, the contribution to the observed anisotropy that originates in the bulk is expected to be negligible. However, surface Ga and As atoms form dimers along specific crystalline axes. In the extreme case one might expect these dimers to exhibit the selection rule of a diatomic molecule, where for bonding to antibonding transitions the optical absorption occurs only for electric fields polarized along the bond axes. For dimers formed from atoms on the Ga and As sublattices this would result in maximum absorption along $[110]$ and $[\bar{1}10]$, respectively. This capability of suppressing bulk contributions makes RDS very surface sensitive despite

the fact that photons typically penetrate a few hundred angstroms into the bulk.

Our RDS system was mounted on a Varian Gen-II solid-source MBE station. Near-normal optical access was provided by an essentially strain-free quartz window.³² The MBE system is equipped with standard RHEED optics, which were operated at an electron energy of 8 keV. Cr-doped semi-insulating (001) GaAs wafers were used to avoid optical anisotropy arising from the linear electro-optic effect induced by space-charge electric fields.³³ After a standard chemical treatment, samples were mounted on a Mo block with In and transferred into the main chamber through a load lock. The native oxide layer was desorbed at 580 °C in the presence of an As₄ flux.

RDS and RHEED measurements were carried out simultaneously under As₄ fluxes ranging from 10⁻⁹ to 10⁻⁵ Torr beam equivalent pressure (BEP), which is defined as the reading of the ion gauge positioned at the sample location when the temperature of the sample holder is 400 °C, as read by a thermocouple. The substrate temperature was determined by subtracting from the reading of a thermocouple in contact with the sample holder the difference between the reading of the same thermocouple at the time the oxide desorption was observed in RHEED and 580 °C, the known true temperature of oxide desorption.³⁴ Well-defined reconstructed surfaces were prepared by controlling the substrate temperature and the As₄ flux.

III. RESULTS AND DISCUSSION

A. Surface reconstructions on the (001) GaAs surface

The (001) GaAs surface exhibits a wide variety of reconstructions depending on conditions such as temperature or ambient As pressure. The primary reconstructions are (4×2), (2×4), and *c*(4×4), which are characterized by 0, 1, and at least 2 outer layers of As, respectively. The presently accepted models for these reconstructions are shown in Fig. 2. The (2×4) reconstruction has been the most thoroughly studied. Three different forms occur depending on the As coverage. These three are termed the α , β , and γ phases, and can be distinguished by the intensity of the RHEED streaks observed along [110].³⁵ The most stable is the β phase, which consists of a single outer layer of As atoms dimerized along $[\bar{1}10]$, with every fourth dimer missing to satisfy charge neutrality.^{9,36,37} Surface As coverage for the β phase is consequently $\frac{3}{4}$ monolayer (ML), as shown in Fig. 2. At higher temperatures some of these dimers desorb, leading to the α phase, which consists of $\frac{1}{2}$ ML of As. At lower temperatures, an extra $\frac{1}{4}$ ML of As atoms are chemisorbed atop the first layer, breaking the original dimers along $[\bar{1}10]$ and forming antisite dimers along [110]. The resulting phase, which still has the (2×4) LRO, is termed γ . Surface coverage of this γ phase is 1 ML distributed between two outer layers of As.

The *c*(4×4) reconstruction occurs for As coverages higher than that of (2×4)- γ and was first observed by

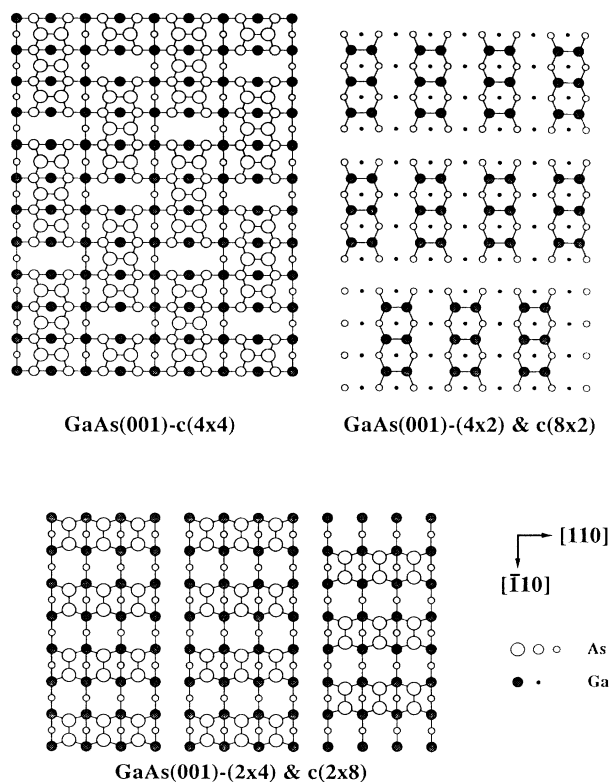


FIG. 2. Presently accepted models of the *c*(4×4), (2×4)/*c*(2×8)- β , and (4×2)/*c*(8×2) reconstructions of (001) GaAs.

Joyce and co-workers.^{1,2,38,39} Based on their RHEED, AES, and angle-resolved photoemission spectroscopy (ARPES) data they propose a model with $\frac{5}{4}$ or $\frac{6}{4}$ ML of outer-layer As with the outermost As layer dimerized along [110]. Recent STM (Ref. 10) and XRD (Ref. 11) studies have shown that the most stable *c*(4×4) reconstructed surface is terminated by $\frac{7}{4}$ ML of As atoms, consisting of an inner full As ML and an outer $\frac{3}{4}$ As ML dimerized along [110], as shown in Fig. 2. Here, the original As dimers of the lower layer have been completely broken to allow bonding of the outermost $\frac{3}{4}$ ML of As. This model also satisfies the charge-neutrality condition.³⁶ Thus the primary difference between the (2×4) and *c*(4×4) reconstructions with respect to the structure of the outer layer is the 90° difference in orientation of the surface As dimers.

The (4×2) reconstruction is formed when the surface As is completely removed, either by desorption at elevated temperature or by depositing Ga on a (2×4) surface. The (4×2) reconstruction consists of $\frac{3}{4}$ ML of Ga dimerized along [110], as also shown in Fig. 2. A number of “transitional” phases such as the (3×1), (4×6), and (1×6) + $\frac{1}{6}nY^*$ (Ref. 6) reconstructions have been reported to exist between (2×4)- α and (4×2). These terminations appear in certain temperature ranges when the As flux is insufficient to form the (2×4) reconstructions. The associated structures are presently uncertain.

B. RD results: Overview

Our results are summarized in Figs. 3–8, which show RD spectra and list the associated RHEED patterns observed as the substrate temperature is slowly varied for different As_4 beam equivalent pressures (BEP's) ranging from 7×10^{-5} Torr (Fig. 3) to mid- 10^{-9} Torr (Fig. 8). Because a long time is required to stabilize effusion from the As cell, data were obtained by varying the substrate temperature at fixed As_4 BEP's.

After desorbing the oxide in an As_4 flux of 10^{-7} to 10^{-5} Torr BEP, the surface reconstruction that is formed exhibits a (2×4) LRO. In this flux regime, the surface is As-rich for substrate temperatures of 600°C or lower. The spectra in Fig. 5, which were obtained under a constant As_4 flux of 2.8×10^{-6} Torr BEP show a typical evolution of the surface as a function of temperature. The 585°C surface exhibited an excellent (2×4) RHEED pattern, and its RD spectrum is identical to that which we have previously reported.²⁶ As the substrate temperature is lowered, both the RD line shape and RHEED pattern stay essentially the same until 500°C . Between 500 and 475°C significant changes occur in the RD line shape, and the reconstruction as observed by RHEED changes from (2×4) to $c(4 \times 4)$. As the temperature is lowered further under these conditions, the RHEED and RD spectra remain qualitatively the same to 189°C and then begin to change again. Below 89°C the flat structure be-

tween 3.5 and 4.3 eV in the RD line shape evolves into a bulge. At the same time the $\frac{1}{2}$ -order streaks along both $[\bar{1}10]$ and $[110]$ in the RHEED pattern weaken with respect to the integer-order streaks, and the background increases.

Before discussing these results in detail, we provide a qualitative framework by pointing out representative RD line shapes associated with the three primary reconstructions: the (2×4) - β phase at 595°C in Fig. 4, the $c(4 \times 4)$ at 473°C in Fig. 5, and the (4×2) at 592°C in Fig. 7. It is clear that the overall line shapes are quite different in the three cases, which means that RDS should be as effective as RHEED in establishing the identity of outer layer reconstructions, even though RDS is sensitive to local electronic structure rather than LRO. The features that will receive the most attention in the following discussion are the positive and negative peaks at 2.5 – 2.8 eV in the (2×4) and $c(4 \times 4)$ spectra, respectively; the 1.8 – 2.1 -eV negative feature in the (4×2) spectrum; and the positive feature in the 4.1 – 4.4 eV energy range that appears in most spectra.⁴⁰

C. (2×4) - α and (2×4) - β reconstructions

As mentioned in Sec. III A, the (2×4) reconstruction can be subdivided into three phases α , β , and γ , which consist of $\frac{1}{2}$, $\frac{3}{4}$, and 1 ML of outer layer As, respectively. These phases can be distinguished by the intensity of the

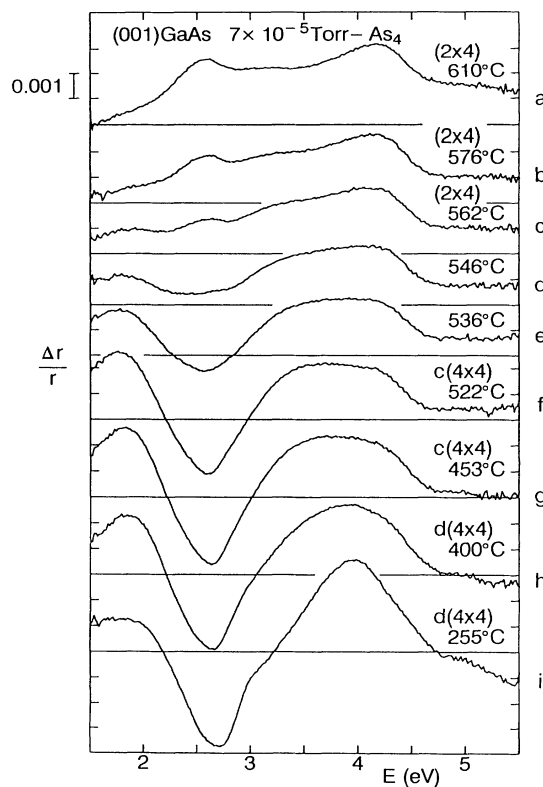


FIG. 3. RD spectra $\Delta r/r = 2 \text{Re}\{(\bar{r}_{\bar{1}10} - \bar{r}_{110})/(\bar{r}_{\bar{1}10} + \bar{r}_{110})\}$ of an MBE-prepared (001) GaAs surface in UHV, obtained as the substrate temperature was lowered from 610°C to 255°C in an As_4 flux of 7×10^{-5} Torr BEP.

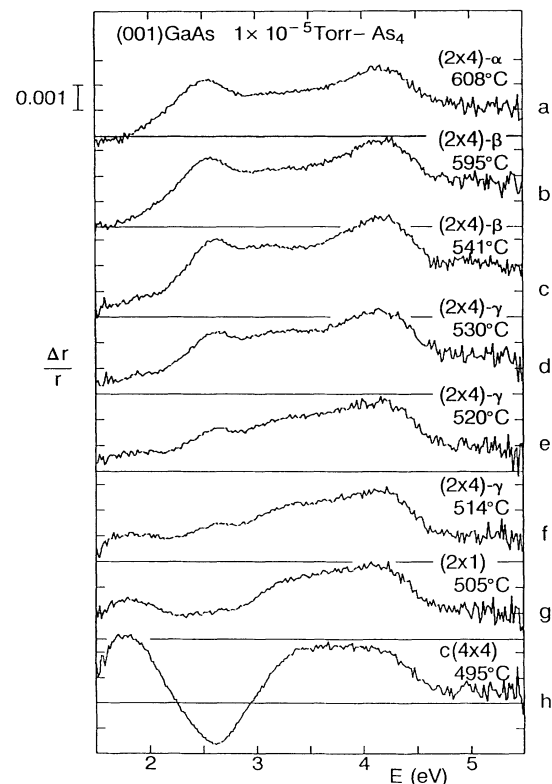


FIG. 4. RD spectra of a (001) GaAs surface in UHV, obtained as the substrate temperature was lowered from 608°C to 495°C in an As_4 flux of 1×10^{-5} Torr BEP.

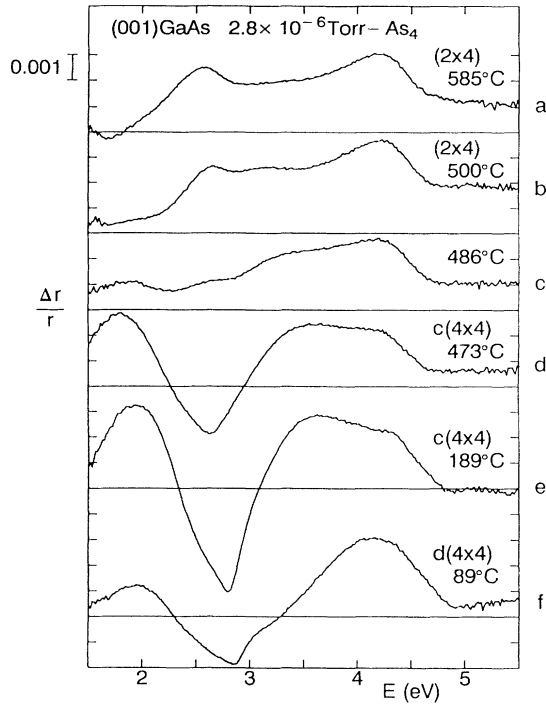


FIG. 5. RD spectra of a (001) GaAs surface in UHV, obtained as the substrate temperature was lowered from 585°C to 89°C in an As_4 flux of 2.8×10^{-6} Torr BEP.

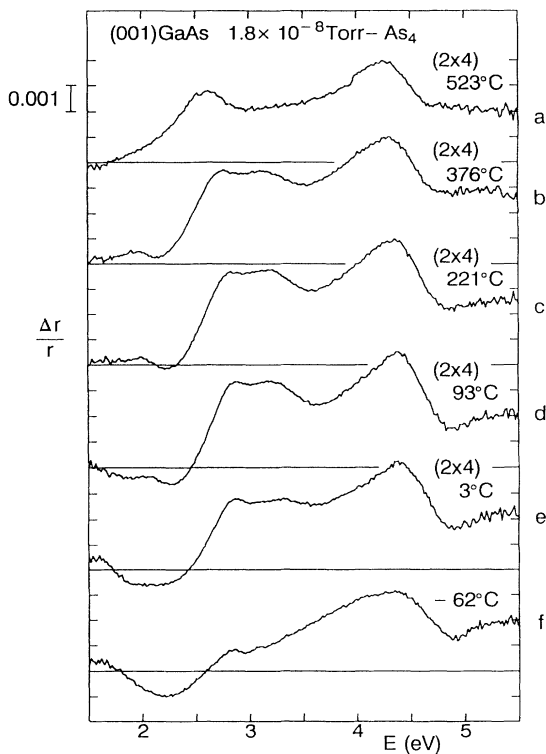


FIG. 6. RD spectra of a (001) GaAs surface in UHV, obtained as the substrate temperature was lowered from 523°C to -62°C in an As_4 flux of 1.8×10^{-8} Torr BEP.

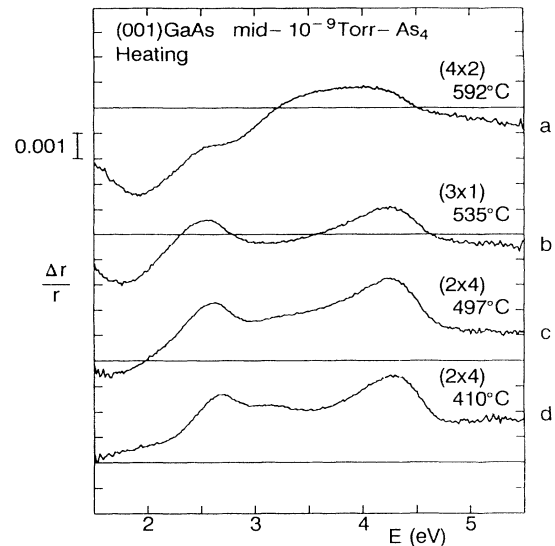


FIG. 7. RD spectra of a (001) GaAs surface in UHV, obtained as the substrate temperature was raised from 410°C to 592°C in a residual As_4 flux of mid- 10^{-9} Torr BEP.

RHEED streaks.³⁵ Here, we show that these phases can also be distinguished by RDS. The relevant spectra are shown in Fig. 4 and were obtained with an As_4 flux of 1×10^{-5} Torr BEP. We consider first the α and β phases, which are characterized by only one outer layer of As and are thus distinct from the γ phase, which we will discuss later together with the $c(4 \times 4)$. Under these conditions the surface maintains the β phase between 541 and 595°C. The β -phase spectra in Fig. 4 are characterized by the positive structures at 2.5–2.8 and 4.1–4.4 eV. The origins of these features have been investigated theoret-

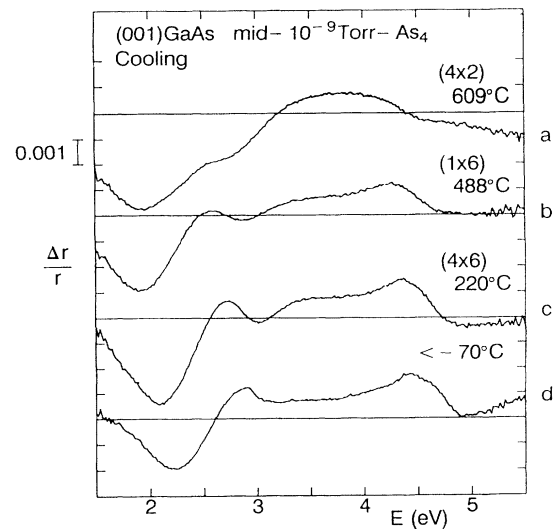


FIG. 8. RD spectra of a (001) GaAs surface in UHV, obtained as the substrate temperature was lowered from 609°C to < -70°C in a residual As_4 flux of mid- 10^{-9} Torr BEP.

cally by Chang and co-workers^{41,42} in a (2×1) model, a reconstruction that is equivalent to (2×4) - β , except that it has no missing dimers. Their tight-binding calculations showed that the 2.5–2.8-eV peak is due to transitions between filled As lone-pair states and unoccupied As-As dimer antibonding orbitals. The 4.1–4.4-eV peak is due to transitions between bonding and antibonding orbitals. In particular, the 2.5–2.8-eV feature is uniquely associated with surface dimers and can therefore be used as a measure of their presence.

When the temperature is increased above 595 °C a net loss of As dimers occurs. This results in a conversion to the α phase, where the surface is terminated by $\frac{1}{2}$ ML of As.³⁵ This is seen in the spectra as a weakening of the two RD features related to As dimers (note that overall signal in the 595 °C spectrum of Fig. 4 is scaled down in the 608 °C spectrum). Further heating is accompanied by additional loss of As, with the surface evolving first to a (3×1) and finally to a (4×2) reconstruction that exhibits Ga dimer spectral features, as will be discussed below. In this range the balance between As desorption and adsorption is delicate, so the α phase is observed only over a relatively narrow temperature range.

D. As-rich (2×4) - γ , $c(4 \times 4)$, and $d(4 \times 4)$ reconstructions

When the temperature is decreased below 541 °C the surface chemisorbs a partial second layer of As atoms. These “antisite” As atoms form dimers along $[110]$ and simultaneously break the underlying dimers along $[\bar{1}10]$. This process is completed with the formation of the $c(4 \times 4)$ reconstruction, which as stated above is $\frac{3}{4}$ ML of As distributed as “antisite” As dimers oriented along $[110]$ atop a full ML of As (Fig. 2). The evolution from (2×4) - β is thus characterized by an increasing concentration of As dimers rotated 90° with respect to those of the (2×4) - β reconstruction. To the extent that the largely intraatomic lone-pair-to-dimer transition at 2.5–2.8 eV is independent of the identity of the substrate atoms on which the dimers reside, the accumulation of “atop” dimers is expected to result in a partial cancellation of the As dimer contribution to the RDS signal at 2.5–2.8 eV. This is already evident in the 530 °C spectrum of Fig. 4. When the sample is cooled to 514 °C, the cancellation is almost complete. At this stage a typical RHEED pattern for the γ phase is also observed. These results are direct evidence for the validity of the “atop” model,³⁵ where the γ phase is interpreted as consisting of a single second-layer As dimer chemisorbed to four of the first-layer As atoms. The formation of an “atop” dimer destroys two of the three original dimers of the first layer in the unit cell, with the single remaining dimer along $[\bar{1}10]$ in principle cancelling the contribution of the atop dimer oriented along $[110]$. This should lead to the elimination of the 2.5–2.8 eV feature as observed in Fig. 4. As with the case involving the 0-to-1 layer transition at higher temperatures, in this temperature regime the balance between chemisorption and desorption at the 1-to-2 layer transition is also delicate, resulting in a relatively narrow range of existence for the γ phase.

When the temperature is lowered further, chemisorp-

tion dominates desorption and the LRO as seen by RHEED evolves to $c(4 \times 4)$. Under these conditions the RD feature at 2.5–2.8 eV reemerges but with the opposite sign. Also, new structures begin to appear at 1.8 eV and between 3.5 and 4.3 eV, and the small feature at 3.0–3.2 eV seen in the γ phase increases its strength. It is worthwhile to note that the surface dielectric anisotropy spectrum of the γ phase also showed a small feature near 3.0 eV.⁴³ We believe this is related to an electronic transition of additional As dimers in antisite positions on top layer.

In an As_4 flux of 2.8×10^{-6} Torr BEP the $c(4 \times 4)$ features sharpen and strengthen to temperatures down to about 190 °C, as seen in Fig. 5. However, at lower temperatures the relatively flat region between 3.5 and 4.2 eV develops into a broad peak. At the same time the RHEED pattern, although qualitatively remaining $c(4 \times 4)$, exhibits increased background and weaker half-order streaks along both $[\bar{1}10]$ and $[110]$. Based on this observation we term the surface termination giving rise to this new RD line shape a disordered $c(4 \times 4)$, or $d(4 \times 4)$, reconstruction.^{27,28}

Further insight into the origin and nature of the $c(4 \times 4)$ and $d(4 \times 4)$ reconstructions is obtained by examining similar data obtained at higher As_4 BEP's. Data for our highest As_4 BEP, 7×10^{-5} Torr, are shown in Fig. 3. This flux is approximately 30 times greater than that used to obtain the data shown in Fig. 5. We note first that (001) GaAs under either condition exhibits a well-defined (2×4) reconstruction, although as could be expected the (2×4) - γ “crossover” phase occurs at the substantially higher temperature of 562 °C for the higher As flux as compared to 486 °C in Fig. 5. Also, the $c(4 \times 4)$ spectrum at 522 °C in Fig. 3 is similar to that obtained at 473 °C in Fig. 5.

However, when sample temperatures are lowered further with higher As_4 flux significant differences are observed. None of the spectra obtained for $c(4 \times 4)$ surfaces at temperatures 453 °C or below in Fig. 3 agrees with any of those at 473 °C or below in Fig. 5. Specifically, the “flat-top” version of the $c(4 \times 4)$ RD spectrum, where the anisotropy is essentially constant between 3.5 and 4.5 eV, occurs over a wide temperature range (473–189 °C) only for relatively low As_4 fluxes. As the As_4 flux is increased, the temperature range over which the “flat-top” spectrum is observed is substantially reduced. We argue that this is due to the following reason. At low fluences we expect the surface reconstruction to be determined by thermodynamics rather than kinetics because the As exchange rate between surface and ambient is low and it is relatively easy for the surface to reach equilibrium. The fact that the flat-top line shape is observed to be stable over a wide temperature range in moderate As_4 flux suggests that the corresponding surface is also relatively stable. For this reason, we assign the flat-top spectrum to the ideal $c(4 \times 4)$ model of Fig. 2. If the As_4 flux is increased or the substrate temperature lowered, then the surface will adsorb excess As on this “ideal” $c(4 \times 4)$. While charge neutrality would seem to prohibit chemisorption of this extra As, if the As_4 arrival rate is high enough and/or the temperature is low enough, then we

expect kinetics to override thermodynamics and allow the surface to become less well ordered. The extra degrees of freedom created by the disorder are expected to make the charge-balance arguments in their simplest form inapplicable. We note that disorder will also be expected at low temperatures where mobility of atoms at surface is low. This is consistent with the "disordered" interpretation of the $d(4\times 4)$ phase.^{27,28} Since the structure is forced by kinetics rather than thermodynamics, we do not expect the atomic arrangements of this surface to be unique. Consistent with this reasoning, $d(4\times 4)$ spectra show variations.

At first sight, the above assignment appears not to be consistent with the XRD results, which suggested that $c(4\times 4)$ is a mixed phase of regions covered by $\frac{7}{4}$ and $\frac{6}{4}$ ML of As.¹¹ However, the stability of $\frac{6}{4}$ ML As-covered $c(4\times 4)$ has not yet been established; the simulation performed in Ref. 11 did not consider other possibilities. In addition, the XRD measurements were carried out after transferring the sample from an MBE chamber to another UHV chamber where As_4 was not supplied. Therefore, while the $c(4\times 4)$ reconstruction with $\frac{6}{4}$ ML As undoubtedly exists, it may be a transitional stage. These surfaces need to be studied in more detail, possibly by STM.

When the As_4 flux was reduced to 10^{-8} – 10^{-9} Torr BEP, we found it impossible to generate a $c(4\times 4)$ reconstruction even at extremely low temperatures. Figure 6 shows RD spectra taken at various temperatures in an As_4 flux of 1.8×10^{-8} Torr BEP. Near 500°C, the existence of a (2×4) - β reconstruction identical to those obtained with higher As_4 BEP was confirmed by both RDS and RHEED. The (2×4) LRO remained until the sample was cooled to 3°C, as observed by RHEED. Between 376 and 3°C, the RD spectra also exhibit the essential features of (2×4) with the addition of an extra structure around 3.4 eV, which indicates the presence of "atop" or "antisite" As dimers along [110] at these relatively low temperatures, as discussed in Sec. III C. At -62°C the reconstruction can no longer be identified by RHEED. The corresponding RD spectrum does not show agreement with those of the (2×4) or $c(4\times 4)$ surfaces, or their intermediates, suggesting that this structure is disordered. We speculate that in As_4 flux of 10^{-8} Torr BEP the surface can convert from (2×4) - β to a disordered structure without intervening (2×4) - γ and $c(4\times 4)$ steps if desorption dominates chemisorption until the temperature becomes so low that desorption ceases and adsorption occurs without diffusion or cracking of As_4 . In fact, the accumulated As is likely to be amorphous As, which is used for capping and typically deposited at or below this temperature.⁴⁴

E. Ga-rich (4×2) , (3×1) , (1×6) , and (4×6) reconstructions

When this As-capped sample is heated in this reduced As flux of mid- 10^{-9} Torr BEP, the (2×4) reconstruction is recovered at -30°C and exists with slight quantitative variations up to about 500°C, as shown in Fig. 7. Near 500°C the entire spectrum starts shifting towards nega-

tive values. RHEED patterns indicate that the surface reconstruction becomes (3×1) at 535°C and (4×2) at 590°C. The (4×2) surface, which consists of Ga dimers formed along [110] with every fourth dimer missing (Fig. 2), exhibits an RD spectrum that is characterized by the prominent negative feature at 1.8–2.1 eV. On the basis of theoretical calculations, this structure has been assigned to electronic excitations between bonding Ga dimer orbitals and empty Ga lone-pair states.^{26,40,41} The (3×1) spectrum shows both sets of features, the negative dip at 1.8–2.1 eV and the peaks at 2.5–2.8 eV and 4.1–4.4 eV, which indicate the presence of both Ga and As dimers.

Consequently, as the (2×4) surface desorbs As upon heating, the underlying Ga atoms rearrange to form surface dimers. At 535°C the process is not very fast and possibly also involves diffusion of remaining As atoms or dimers. Judging by the evolution of the intensities of the 2.5–2.8 and 4.1–4.4-eV features, the (3×1) structure is clearly an intermediate phase with less than $\frac{3}{4}$ ML coverage of As. In fact, the As coverage is possibly less than $\frac{1}{2}$ ML because the structure is prepared by heating the (2×4) - α surface. We note here that the (3×1) structure is obtained only during the transition from (2×4) - α to (4×2) , and not during the reverse process, as will be discussed below. This indicates that the (3×1) reconstruction may not be thermodynamically stable and can only be reached through appropriate kinetic pathways. The vagueness of the associated RHEED pattern indicates that the structure is not well ordered.

However, the (3×1) surface can be reproducibly and stably achieved during MBE growth and is in fact the preferred surface termination for growth of certain structures, for example, $GaAs-Al_xGa_{1-x}As$ quantum wells on channeled-substrate (001) GaAs.⁴⁵ It is well known that selective growth allows multiquantum-well (MQW) laser structures to be grown by OMCVD on ridges and grooves isolated by $(m11)A$ side facets. However, with MBE, until recently, growth rates on different orientations were considered to be merely a function of the normal flux. But Meier *et al.* reported that, under the (3×1) stabilized condition with a low $As_4:(Ga,Al)$ flux ratio of 0.9 and a growth rate of 1.25 $\mu\text{m/h}$, such structures can also be grown by MBE.⁴⁵ They showed that growth interruption at a high growth temperature of 700°C can enhance migration of Ga from $(m11)A$ to (001) planes. As a result, MQW laser structures isolated by $Al_xGa_{1-x}As$ can be obtained. A RHEED study of the growth properties of GaAs and AlAs on high-index (117) and (119) surfaces supported this interpretation.⁴⁶ However, a more detailed study on the surface diffusion length of Ga on (001) GaAs by scanning microprobe RHEED by Hata, Watanabe, and Isu showed that the diffusion length is not determined merely by the temperature but also by the surface reconstruction.⁴⁷ They showed that the diffusion length increases drastically when the surface reconstruction converts from (2×4) to (3×1) . They attributed this to the difference in surface density of As atoms, since these would normally capture Ga. At the same time Tsao and co-workers investigated the reactive sticking of As_4 onto variously reconstructed

(001) GaAs surfaces, and demonstrated that this coefficient is not merely a function of surface As coverage but shows a maximum at the (3×1) reconstruction as the surface converts from (2×4) to (4×2) .⁴⁸ The (3×1) structure needs to be established in detail, as it shall provide considerable insights concerning these interesting topics.

By increasing the temperature, the (3×1) surface desorbs the remaining As and converts to the Ga-terminated (4×2) reconstruction. If this (4×2) surface is cooled in an almost complete absence of As, a different set of reconstructions is observed, resulting in a hysteresis effect. This is illustrated in Fig. 8, which presents spectra obtained in a background As_4 pressure of mid- 10^{-9} Torr BEP. When the (4×2) surface is cooled to 488°C , the surface evolves to a $(1 \times 6) + \frac{1}{6}nY^*$ reconstruction,⁶ which is probably identical to the (6×6) reconstruction initially reported by Cho.³ Recent studies by Palmström and co-workers⁴⁹ have revealed that this reconstruction can be generated in the absence of an As_4 flux by raising the substrate temperature above that where the (3×1) reconstruction would ordinarily occur, and that it is distinct from (4×6) , especially when observed by LEED. From their LEED observations Bachrach *et al.* also concluded that (4×6) is not a mixture of (4×1) (Ref. 50) and (1×6) (Ref. 51), which agrees with the result of van Bommel, Crombeen, and Oirschot.⁶ By cooling the substrate to 200°C , the surface converts to (4×6) . General features of the RD spectra for (1×6) and (4×6) are similar to those obtained for (3×1) [compare Figs. 7 and 8]. The primary difference occurs between 3.0 and 3.5 eV. The (1×6) and (4×6) spectra show a small rise in this energy regime, while the (3×1) spectrum shows a shallow dip.

Although the (3×1) , (1×6) , and (4×6) phases have been well studied, their associated atomic structures are still uncertain. Our RDS observations suggest that the (1×6) and (4×6) surfaces are mixtures of regions terminated by As and Ga dimers, and the LRO detected by RHEED or LEED is a measure of the conditions under which the surface was prepared. If dimers were the only contributors to the RD features, then the (1×6) and (4×6) spectra should be representable as linear combinations of (2×4) and (4×2) spectra. We show a result of this attempt in Fig. 9. The quantitative agreement between the (1×6) spectrum and any of the linear combinations of (2×4) and (4×2) is poor, showing that other factors are involved. [Note that (3×1) and (4×6) spectra do not agree with any of these linear combinations either]. The discrepancy may be due to boundaries between these areas and/or the perturbation of the surface electronic structure by LRO.

The (3×1) , (1×6) , and (4×6) structures only result when the As flux is insufficient to form the (2×4) - β reconstruction. The (3×1) is a transient structure that is formed from (2×4) - β when the As_4 supply rate is sufficiently low. Since under sufficient As_4 flux (2×4) - β is stable in the 500 – 600°C range, the formation of (3×1) involves both As desorption and diffusion. On the other hand, (1×6) and (4×6) are formed only when a Ga-terminated surface is cooled in a very low supply of As_4 .

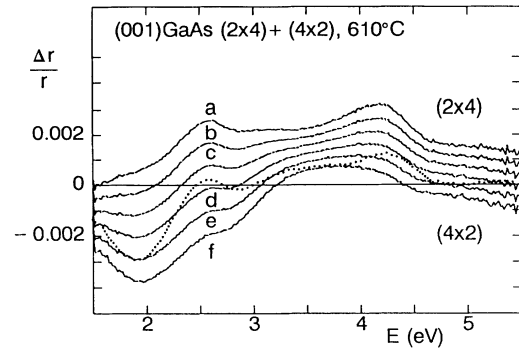


FIG. 9. RD spectra synthesized from linear combinations of (2×4) and (4×2) spectra at 610°C : (a) pure (2×4) , (b) $(2 \times 4)_{0.8}(4 \times 2)_{0.2}$, (c) $(2 \times 4)_{0.6}(4 \times 2)_{0.4}$, (d) $(2 \times 4)_{0.4}(4 \times 2)_{0.6}$, (e) $(2 \times 4)_{0.2}(4 \times 2)_{0.8}$, and (f) pure (4×2) . (a) and (f) are data also shown in Figs. 3 and 8, respectively. The dotted line is the RD spectrum of the (1×6) reconstruction at 488°C in Fig. 8.

Assuming that As desorption rates depend mainly on temperature, and noting that these reconstructions can form only if the As supply rate exceeds the desorption rate, this implies substrate temperatures low enough so that the surface diffusion rate is small. Consequently, the thermodynamically stable phase is (2×4) - β . By supplying As_4 flux of 10^{-6} Torr BEP at a substrate temperature of 430°C , the surface becomes $c(4 \times 4)$, which of course becomes (2×4) - β when the temperature is raised.

The origins of some of the features that appear in these spectra are not yet clear, but further theoretical work is expected to determine them. Nevertheless, these spectra, all of which are correlated to RHEED observations, are highly reproducible and consequently allow RDS to be used to determine (001) GaAs surface reconstructions in both UHV and non-UHV environments. To our knowledge this is the first time that an optical spectroscopy has been successfully employed for the detailed structural analysis of surfaces.

F. Phase diagram and implications for crystal growth

The determination of which surface reconstructions are present during growth is important because it provides us with information on the kinetics and mechanism of growth, and consequently better control over the material. We note also that, since the different reconstructions are associated with different surface energies, control over surface reconstructions provides a certain measure of control over, for example, spontaneous ordering, dopant incorporation, etc., without need to introduce foreign species as surfactants. As a first step towards a complete phase diagram and to obtain a systematic picture of the As-terminated surfaces, we mapped the distribution of the (2×4) and $c/d(4 \times 4)$ classes of reconstructions as a function of temperature and As incorporation rate in Arrhenius form, as shown in Fig. 10. The dots, crosses, and open circles represent (2×4) , $c/d(4 \times 4)$, and marginal structures, respectively, where marginal structures are those where the RHEED pattern indicated

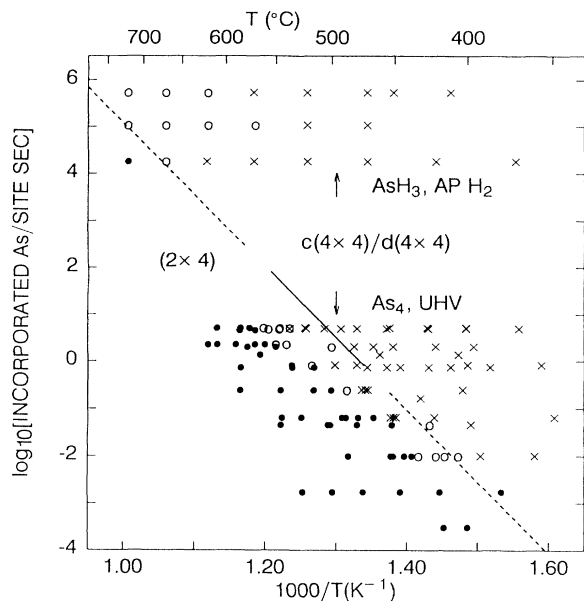


FIG. 10. Summary of (001) GaAs structures observed as a function of substrate temperature and As supply rate in the absence of Ga supply, shown in Arrhenius form. For As_4 , the flux is converted into an As incorporation rate from RHEED measurements, as described in Ref. 28. For AsH_3 , the incorporation rate is established from thermodynamic data as also described in Ref. 28. Ambient conditions are UHV for As_4 and AP H_2 for AsH_3 . Dots, crosses, and open circles represent (2×4) , $c/d(4 \times 4)$, and marginal structures, respectively, as established by RDS and RHEED for UHV and by RDS for AP H_2 . The solid line is the phase boundary established in Ref. 52.

that conversion of superstructure from one to the other and the RD spectra could not be categorized as either of the two. This is the first optically determined phase diagram for growth surfaces.

A number of phase diagrams have previously been established by RHEED,^{51–54} and they are all in reasonably good agreement with our present data.⁵⁵ A very detailed RHEED-determined phase diagram is in fact given in Ref. 54. Van Hove, Cohen, and Lent established a boundary between (2×4) and $c(4 \times 4)$ by RHEED on MBE-prepared surfaces in UHV (Ref. 52) under conditions similar to ours, that is, under As_4 flux without Ga. Their result is shown by a straight line in Fig. 10. Our results are in good agreement. From the slope of this boundary, we estimate a chemisorption enthalpy of 70.2 kcal/mol (3.0 eV/molecule) for As_4 on the (2×4) surface.

Our recent work on (001) GaAs surfaces during OMCVD growth^{27,28} has shown that surface reconstructions similar to those that exist in UHV exist even at atmospheric pressure. LRO's observed by XRD under near atmospheric pressure static conditions also supports our results.⁵⁶ This result is extremely significant, because all previous models of OMCVD growth were based on the assumption that surface structures in non-UHV environments are totally different from those in UHV because clean surfaces in UHV are highly reactive and readily contaminated. This major, and in this case, incorrect as-

sumption is a common one made by surface scientists for understanding surfaces in non-UHV ambients. In a larger sense, the fact that reconstructions do exist in non-UHV environments justifies the applicability of results of UHV surface science to non-UHV surface science.

We have shown that this (2×4) - $c/d(4 \times 4)$ boundary also extends into the OMCVD regime, where As is supplied as AsH_3 in an AP H_2 ambient. The results are also given in Fig. 10. Together with the RD spectra that we previously reported for the OMCVD-prepared surfaces, this provides further evidence that the surface reconstructions of (001) GaAs in AP H_2 are similar, possibly identical, to those in UHV.^{27,28} Moreover, we found that under conditions where OMCVD growth is actually carried out, the AsH_3 stabilized surfaces exhibits the $d(4 \times 4)$ -like reconstruction in contrast to the (2×4) , which is the standard conditions in MBE.⁵⁷ We believe that this difference in reconstruction during growth is important in elucidating the mechanism of OMCVD, atomic layer epitaxy in particular.⁵⁸

The recent apparent contradiction with XRD results that failed to detect surface reconstructions during OMCVD growth,⁵⁶ when Ga- and As-containing precursors are codeposited, allows us to emphasize the characteristics that distinguish RDS from more conventional surface-analytic techniques. We recall that RDS is sensitive to local electronic structure rather than LRO. Therefore, RDS provides us with complementary information with respect to that obtained by diffraction techniques such as RHEED or XRD. For instance, by combining our results on OMCVD with those of Ref. 56, one possible conclusion is that the surface during OMCVD growth reconstructs to form dimers but does not order sufficiently to exhibit LRO.⁵⁹ Consequently, under conditions where surfaces do not form superstructures, RDS is the more informative probe. For example, Farrell and Palmström³⁵ proposed a model for the transition between (2×4) and $c(4 \times 4)$ where excess As dimers oriented along $[110]$ start adsorbing on the surface, thereby breaking dimers oriented along $[\bar{1}10]$. Based on their model, As dimers begin to form along $[110]$, while the LRO remains (2×4) . This distinction cannot be made from RHEED due to the discrete nature of reconstruction changes. In contrast, RD can both detect and measure such changes in a continuous and quantifiable manner, and our present data clearly support this model. At the crossover between (2×4) and $c(4 \times 4)$, the RD spectra show more drastic changes than the RHEED patterns. For example, in the 485–470 °C range RD responds immediately to the structural change on the surface (see Fig. 1), while the RHEED pattern converts to $c(4 \times 4)$ very slowly. This is clearly due to the time lag between the formation of As dimers along $[110]$ and the formation of their LRO to which RHEED is sensitive. This also shows that RDS specifically, and optical probes more generally, will be very useful for studying surface dynamics, which may also involve metastable structures that may often not have time to develop LRO in the time frames of interest. Dynamical studies of surface reactions on (001) GaAs in various environments are underway.

IV. CONCLUSION

We have performed simultaneous RD and RHEED measurements on (001) GaAs surfaces in UHV to establish a data base of RD spectra for (001) GaAs. Specifically, we have determined RD spectra for $(2 \times 4)\text{-}\alpha$, $(2 \times 4)\text{-}\beta$, $(2 \times 4)\text{-}\gamma$, $c(4 \times 4)$, $d(4 \times 4)$, (4×2) , (3×1) , (1×6) , and (4×6) reconstructions in UHV. The comparison between RD and RHEED data under dynamic conditions clearly illustrates their complementari-

ty, with RDS establishing the kinetics of dimer formation and RHEED and their LRO. Work on non-UHV surfaces based on the present results are underway.

ACKNOWLEDGMENTS

The authors thank C. J. Palmstøm for fruitful discussions. One of us (I.K.) acknowledges financial support from the Office of Naval Research under Contract No. N-00014-90-J-1267.

*Present address: IRC for Semiconductor Materials, Imperial College, London SW7 2BZ, UK.

[†]Present address: Department of Physics, North Carolina State University, Raleigh, NC 27695-8202.

¹J. H. Neave and B. A. Joyce, *J. Cryst. Growth* **44**, 387 (1978).

²P. K. Larsen, J. H. Neave, J. F. van der Veen, P. J. Dobson, and B. A. Joyce, *Phys. Rev. B* **27**, 4966 (1983).

³A. Y. Cho, *J. Appl. Phys.* **47**, 2841 (1976).

⁴A. Y. Cho and J. R. Arthur, *Prog. Solid State Chem.* **10**, 157 (1975).

⁵P. Drathen, W. Ranke, and K. Jacobi, *Surf. Sci.* **77**, L162 (1978); W. Ranke and K. Jacobi, *Prog. Surf. Sci.* **10**, 1 (1981).

⁶A. J. van Bommel, J. E. Crombeen, and T. G. J. van Oirschot, *Surf. Sci.* **72**, 95 (1978).

⁷P. K. Larsen, J. H. Neave, and B. A. Joyce, *J. Phys. C* **14**, 167 (1981).

⁸T.-C. Chiang, R. Ludeke, M. Aono, G. Landgren, F. J. Himpsel, and D. E. Eastman, *Phys. Rev. B* **27**, 4770 (1983).

⁹M. D. Pashley, K. W. Haberern, W. Friday, J. M. Woodall, and P. D. Kirchner, *Phys. Rev. Lett.* **60**, 2176 (1988).

¹⁰D. K. Biegelsen, R. D. Bringans, J. E. Northrup, and L.-E. Swartz, *Phys. Rev. B* **41**, 5701 (1990).

¹¹M. Sauvage-Simkin, R. Pinchaux, J. Massies, P. Calverie, N. Jedrecy, J. Bonnet, and I. K. Robinson, *Phys. Rev. Lett.* **62**, 563 (1989).

¹²N. D. Lang, *Phys. Rev. Lett.* **58**, 45 (1987).

¹³R. J. Wilson and S. Chiang, *Phys. Rev. Lett.* **58**, 369 (1987).

¹⁴R. Tromp, R. J. Hamers, and J. E. Demuth, *Phys. Rev. Lett.* **58**, 373 (1987).

¹⁵J. A. Stroschio, R. M. Feenstra, and A. P. Fein, *Phys. Rev. Lett.* **58**, 1668 (1987).

¹⁶Y. Hasegawa, I. Kamiya, T. Hashizume, T. Sakurai, H. Tochihara, M. Kubota, and Y. Murata, *Phys. Rev. B* **41**, 9688 (1990).

¹⁷D. E. Aspnes, J. P. Harbison, A. A. Studna, and L. T. Florez, *J. Vac. Sci. Technol. A* **6**, 1327 (1988).

¹⁸D. E. Aspnes, E. Colas, A. A. Studna, R. Bhat, M. A. Koza, and V. G. Keramidas, *Phys. Rev. Lett.* **61**, 2782 (1988).

¹⁹D. E. Aspnes, R. Bhat, E. Colas, V. G. Keramidas, M. A. Koza, and A. A. Studna, *J. Vac. Sci. Technol. A* **7**, 711 (1988).

²⁰A. J. Pidduck, D. J. Robbins, A. G. Cullis, D. B. Gasson, and J. L. Glasper, *J. Electrochem. Soc.* **136**, 3083 (1989); A. J. Pidduck, D. J. Robbins, D. B. Gasson, C. Pickering, and J. L. Glasper, *ibid.* **136**, 3088 (1989).

²¹Y. Horikoshi, H. Yamaguchi, F. Briones, and M. Kawashima, *J. Cryst. Growth* **105**, 326 (1991).

²²D. E. Aspnes, *Proc. SPIE* **946**, 112 (1988); D. E. Aspnes, W. E. Quinn, and S. Gregory, *Appl. Phys. Lett.* **57**, 2707 (1990).

²³T. Stehlin, M. Feller, P. Guyot-Sionnest, and Y. R. Shen, *Opt. Lett.* **13**, 389 (1988); M. E. Pemble, D. S. Buhaenko, S. M.

Francis, P. A. Goulding, and J. T. Allen, *J. Cryst. Growth* **107**, 37 (1991); J. A. Prybyla, H. W. K. Tom, and G. D. Ammiller, *Phys. Rev. Lett.* **68**, 503 (1992).

²⁴Y. R. Shen, *Nature* **337**, 519 (1989).

²⁵Y. J. Chabal, G. S. Higashi, K. Raghavachari, and V. A. Burrows, *J. Vac. Sci. Technol. A* **7**, 2104 (1989); L. P. Sadwick, K. L. Wang, D. L. Joseph, and R. F. Hicks, *ibid.* **7**, 273 (1989); A. V. Annapragada, S. Salim, and K. F. Jensen, in *Atomic Layer Growth and Processing*, edited by T. F. Kuech, P. D. Dapkus, and Y. Aoyagi, MRS Symposia Proceedings No. 222 (Materials Research Society, Pittsburgh, 1991), p. 81.

²⁶M. Wassermeier, I. Kamiya, D. E. Aspnes, L. T. Florez, J. P. Harbison, and P. M. Petroff, *J. Vac. Sci. Technol. B* **9**, 2263 (1991).

²⁷I. Kamiya, D. E. Aspnes, H. Tanaka, L. T. Florez, J. P. Harbison, and R. Bhat, *Phys. Rev. Lett.* **68**, 627 (1992).

²⁸I. Kamiya, H. Tanaka, D. E. Aspnes, L. T. Florez, E. Colas, J. P. Harbison, and R. Bhat, *Appl. Phys. Lett.* **60**, 1238 (1992).

²⁹I. Kamiya, H. Tanaka, and D. E. Aspnes, *Bull. Am. Phys. Soc.* **36**, 644 (1991).

³⁰D. E. Aspnes, E. Colas, A. A. Studna, R. Bhat, M. A. Koza, and V. G. Keramidas, *Vacuum* **41**, 978 (1990).

³¹J. D. E. McIntyre and D. E. Aspnes, *Surf. Sci.* **24**, 417 (1971).

³²A. A. Studna, D. E. Aspnes, L. T. Florez, J. P. Harbison, and R. Ryan, *J. Vac. Sci. Technol. A* **7**, 3291 (1989).

³³H. Tanaka, E. Colas, I. Kamiya, D. E. Aspnes, and R. Bhat, *Appl. Phys. Lett.* **59**, 3443 (1991); S. E. Acosta-Ortiz and A. Lastras-Martínez, *Solid State Commun.* **64**, 809 (1987); *Phys. Rev. B* **40**, 1426 (1989).

³⁴A. Y. Cho, *Thin Solid Films* **100**, 291 (1983); A. J. SpringThorpe, S. J. Ingey, B. Emmerstorfer, and P. Mandeville, *Appl. Phys. Lett.* **50**, 77 (1987); T. Mizutani, *J. Vac. Sci. Technol. B* **6**, 1671 (1988).

³⁵H. H. Farrell and C. J. Palmstøm, *J. Vac. Sci. Technol. B* **8**, 903 (1990).

³⁶H. H. Farrell, J. P. Harbison, and L. D. Peterson, *J. Vac. Sci. Technol. B* **5**, 1482 (1987).

³⁷D. J. Chadi, *J. Vac. Sci. Technol. A* **5**, 834 (1987).

³⁸B. A. Joyce, in *Molecular Beam Epitaxy and Heterostructures*, edited by L. L. Chang and K. Ploog (Nijhoff, Dordrecht, 1985), p. 37.

³⁹J. van der Veen, P. K. Larsen, J. H. Neave, and B. A. Joyce, *Solid State Commun.* **49**, 659 (1984).

⁴⁰The peaks shift as a function of temperature. To avoid confusion we define these peaks allowing these variations and we use these definitions throughout.

⁴¹D. E. Aspnes, Y. C. Chang, A. A. Studna, L. T. Florez, H. H. Farrell, and J. P. Harbison, *Phys. Rev. Lett.* **64**, 192 (1990).

⁴²Y. C. Chang and D. E. Aspnes, *Phys. Rev. B* **41**, 12002 (1990).

⁴³D. E. Aspnes, L. T. Florez, A. A. Studna, and J. P. Harbison,

- J. Vac. Sci. Technol. B **8**, 936 (1990).
- ⁴⁴I. Kamiya, L. T. Florez, D. E. Aspnes, and J. P. Harbison (unpublished).
- ⁴⁵H. P. Meier, E. Van Gieson, P. W. Epperlein, C. Harden, W. Walter, M. Krahl, and D. Bimberg, J. Cryst. Growth **95**, 66 (1989).
- ⁴⁶H. Tsuda and T. Mizutani, J. Cryst. Growth **111**, 88 (1991).
- ⁴⁷M. Hata, A. Watanabe, and T. Isu, J. Cryst. Growth **111**, 83 (1991).
- ⁴⁸T. M. Brennan, J. Y. Tsao, and B. E. Hammons, J. Vac. Sci. Technol. A **10**, 33 (1992).
- ⁴⁹R. Duszak, C. J. Palmstrøm, L. T. Florez, Y.-N. Yang, and J. H. Weaver, J. Vac. Sci. Technol. B **10**, 1891 (1992).
- ⁵⁰ (4×1) is reported to occur under a low As:Ga flux ratio at low temperature (see, for example, Ref. 54) although we did not produce this structure in the present study.
- ⁵¹R. Z. Bachrach, R. S. Bauer, P. Chiaradia, and G. V. Hansson, J. Vac. Sci. Technol. **18**, 797 (1981); **19**, 335 (1981).
- ⁵²J. M. Van Hove, P. I. Cohen, and C. S. Lent, J. Vac. Sci. Technol. A **1**, 546 (1983).
- ⁵³S. M. Newstead, R. A. A. Kubiak, and E. H. C. Parker, J. Cryst. Growth **81**, 49 (1987).
- ⁵⁴L. Däweritz and R. Hey, Surf. Sci. **236**, 15 (1990).
- ⁵⁵Minor discrepancies still remain in the details of the Ga-rich $c(8 \times 2)$, (1×6) , and (4×6) .
- ⁵⁶P. H. Fuoss, D. W. Kisker, G. Renaud, K. L. Tokuda, S. Brennan, and J. L. Kahn, Phys. Rev. Lett. **63**, 2389 (1989); D. W. Kisker, P. H. Fuoss, K. L. Tokuda, G. Renaud, S. Brennan, and J. L. Kahn, Appl. Phys. Lett. **56**, 2025 (1990); F. J. Lamelas, P. H. Fuoss, P. Imperatori, D. W. Kisker, G. B. Stephenson, and S. Brennan, *ibid.* **60**, 2610 (1992).
- ⁵⁷We have also observed using RDS that the reconstruction remains $d(4 \times 4)$ -like even upon codeposition of trimethylgallium and AsH_3 under standard OMCVD growth conditions; H. Tanaka, I. Kamiya, D. E. Aspnes, and R. Bhat (unpublished).
- ⁵⁸I. Kamiya, D. E. Aspnes, H. Tanaka, L. T. Florez, E. Colas, J. P. Harbison, and R. Bhat, Appl. Surf. Sci. **60/61**, 534 (1992); D. E. Aspnes, I. Kamiya, H. Tanaka, and R. Bhat, J. Vac. Sci. Technol. B **10**, 1725 (1992).
- ⁵⁹Another possibility is that conditions, e.g., temperatures and pressures of AsH_3 and TMG, may be different in these experiments. For example, when the As_4 -stabilized surface exhibits a $c(4 \times 4)$ LRO in MBE we have observed that the RHEED oscillation behavior upon Ga deposition depends on how far away the condition is from the (2×4) - $c(4 \times 4)$ phase boundary.

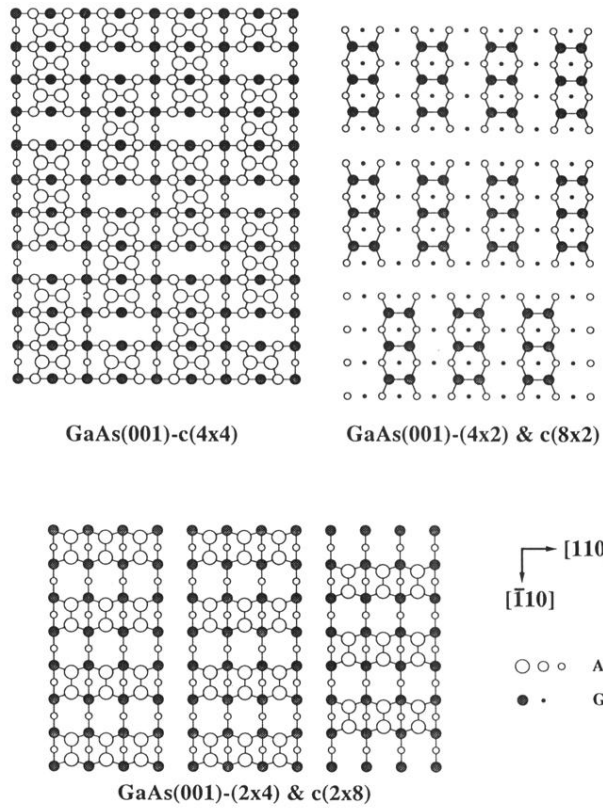


FIG. 2. Presently accepted models of the $c(4 \times 4)$, $(2 \times 4)/c(2 \times 8)$ - β , and $(4 \times 2)/c(8 \times 2)$ reconstructions of (001) GaAs.